A Real-Time Micro-sensor Motion Capture System

Zhang Nan[1], Shunyan Sun[1,2], Jiankang Wu[1,2], Xiaoli Meng[1,2], and Guanhong Tao[1]

[1] Sensor Network and Applications Research Center, Chinese Academy of Sciences, Beijing, China
[2] China-Singapore Institute of Digital Media, Singapore
zhangnan198711@gmail.com, sunshuy09b@mails.gucas.ac.cn, jkwu@gucas.ac.cn

Abstract. Optical human motion capture system can be applied in commercial use, but require expensive studio-like environments which cannot be fulfilled for daily-life use. We present a substitute system: a real-time motion capture system based on micro sensors, which is ubiquity, low-cost and able to reconstruct human motion almost in any environment in real-time. This system consists of three subsystems: a sensor subsystem, a data fusion subsystem and an animation subsystem. Experiments show that our system can reconstruct motions and render animations in real-time, and reach the accuracy of optical human motion capture system

Keywords: Human motion capture, micro-sensor network, data fusion, real-time motion reconstruction.

1 Introduction

Human Motion capture (Mocap) has wide applications in many areas, such as virtual reality, interactive game, sports training and film-making, etc. It has attracted lots of research interests in the last two decades, and a number of Mocap system have been developed, including optical system, mechanical system, inertial system, magnetic system and hybrid system.

Among all the motion capture techniques, optical Mocap is one of the most mature ones, such as Vicon[1]. In optical Mocap, a subject is asked to wear retro-reflective or light emitting markers. Exact 3D locations of these markers are computed from the images which are recorded by certain number of high resolution surrounding cameras, in order to form the motion of the subject. Optical Mocap systems are of their high accuracy and fast update rates. However, they need multiple high speed and high resolution cameras structured and calibrated in a dedicated studio, which restricts applications into a studio-like environment; the systems are quite complex and have the line-of-sight problem.

Mechanical systems, such as Gypsy[2], employ an exoskeleton which is attached to the articulated body segments to measure joint angles by goniometers

R. Wang and F. Xiao (Eds.): CWSN 2012, CCIS 334, pp. 685–694, 2013.

directly. They are transportable and work with any PC for real time performance. However, the main disadvantage of them is that it impedes motion and is uncomfortable to wear for extended time periods[3].

Inertial motion capture systems, such as Verhaert's ALERT system[4], use gyroscopes or accelerometers placed on each body segment to measure orientation. They are portable, and do not have the line-of-sight problem. However, the measurements drift significantly over extended time periods.

Magnetic systems, such as MotionStar[5], use a magnetic field (generated by a magnetic coil or earth magnetic field) to determine both position and orientation of body segments. They can achieve good accuracy in the situation of no interference. However, they have high power consumption and are extremely sensitive to the ferromagnetism in the environment.

Ultrasonic systems, such as Cricket location system[6], employ a set of ultrasonic pulse emitters which are worn by a subject and a set of receivers which are placed at fixed locations in the environment, in order to determine each emitter's location by time-of-flight and triangulation. They are of high tracking accuracy. However, the signal interference is seriously[3,7].

Among all the systems, the research on human motion capture using miniature inertial/magnetic sensors becomes more and more attractive. In Micro-sensor Motion capture (MMocap), miniature inertial and magnetic sensor nodes are attached to body segments. Segment orientation and position can be estimated from the fusion of sensory data. Based on the estimated orientation and position, together with the length of each segment and the arranging relationship between segments, the motion of the whole body can be obtained. MMocap has no line-of-sight requirements, and no emitters to install. Thus, MMocap systems can be applied in a variety of applications almost everywhere. In this paper, we present the design of our ambulatory real-time MMocap system using wearable miniature sensor nodes, which are placed at human body segments. The collected motion signals from micro-sensor nodes are then used to estimate orientations and positions by fusion of sensory data. A sensor data-driven hierarchy human motion model is developed and driven by estimated motion information for real-time motion reconstruction. The experimental results have shown that our motion capture system can capture human motion and drive animation in real-time without drift and delay.

The rest of the paper is organized as follows. Section 2-4 describes the design of the prototype system, including the hardware design and the 3D human motion reconstruction. Particularly, section 4 will discuss the data fusion approach for motion information. And the experimental results will be given in Section 5.

2 Sensor Subsystem

The system of our wearable real-time micro-sensor motion capture is implemented by three subsystems: sensor subsystem, data fusion subsystem and the animation subsystem. As depicted in Figure 1: The sensor subsystem samples and gathers human motion signals, and transmits sensor data to data fusion subsystem. Data fusion subsystem fuses data to obtain the motion information, and sends the motion information to the animation subsystem. The animation subsystem renders animation using an avatar in the 3D virtual space in real-time. The fusion subsystem and the animation subsystem are both implemented in a PC-like terminal which also controls sensor subsystem. The communication between the sensor subsystem and the fusion subsystem is operated wirelessly via Bluetooth or Wi-Fi.

The sensor subsystem is described in this section. Animation subsystem is briefed in section 3. The data fusion subsystem will be discussed in section 4.

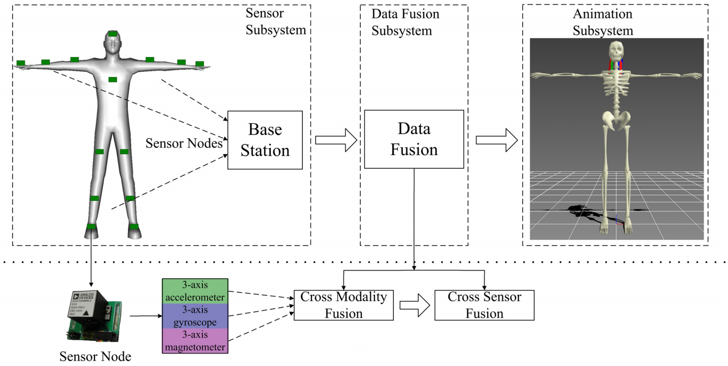

Fig. 1. Our MMocap system contains three subsystems: sensor subsystem, data fusion subsystem and animation subsystem

Sensor subsystem consists of two parts: a base station and certain micro-sensor nodes. Sensor nodes sample human motion signals, and send them to the base station via I^2C protocol. On each body segment a sensor node is fixed. Measurement units on node are MEMS micro-sensors including a triad micro accelerometer, a triad micro magnetometer, and a triad micro gyroscope. The accelerometer measures acceleration data which is mixed with human motion acceleration and earth gravity acceleration. The magnetometer measures local earth magnetic field. The gyroscope measures angular rates. The motion information required by animation system can be filtered from those data in the data fusion subsystem detailed in section 4.

Sensor nodes are wired connected to the base station using shielded cables. The sampling rate can be adjusted according to applications, and up to 200Hz. Rechargeable Li-ion battery pack is used to provide power for the sensor subsystem. Taking the range of human activity and exercise level of comfort into account, the system uses wireless communications to send data between the base station and the data fusion subsystem. Depending on different circumstances, the system uses two different wireless communication protocols: Bluetooth and Wi-Fi, while the former one for indoor applications, and the latter one for outdoor applications.

3 Animation Subsystem

The motion information from the data fusion subsystem will be sent to the animation subsystem to drive an avatar in the 3D virtual space for real-time human motion reconstruction. During the motion reconstruction, an articulated anatomic skeleton human model is utilized to represent the subject's body structure. The model is composed of chains of bone segments linked by joints. It comprises a total of 16 segments. We assume that each bone segment is rigid and their shape does not change during the motion. Each segment has 6 DOFs (degree of freedom), three of them represent position and the other three orientation.

The DOF of the articulated body model is represented by a hierarchical structure. In this structure, body segments keep a parent-child hierarchy relationship, which is maintained by a topological tree as shown in Figure 2. The root of the tree is the pelvis segment, which is also the Center of Mass (CoM) of the avatar. Each segment is the child node of the parent segment, except the root segment. The human model is driven by motion parameters, given by the data fusion subsystem, which results in the real-time animation of human motion. The motion parameters include orientations and positions of body segments.

Animation system may be rendered using OpenGL or D3D technology, or in Maya or OGRE.

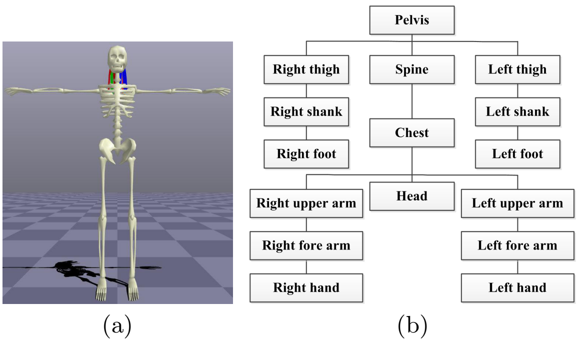

Fig. 2. The hierarchical model of the animation subsystem

4 Data Fusion Subsystem

As mentioned above, on each body segment a sensor node is fixed. The data fusion subsystem receives sensor signals and fuses them to obtain motion information. The motion information mainly includes orientation and position of each body segment.

The data fusion subsystem first performs cross-modality fusion, which estimates orientation quaternions from the three different modalities of sensors. This process is accomplished by the orientation estimation. We use a quaternion to represent the orientation of each body segment. A quaternion consists of a vector part $\boldsymbol{e} = (q_1, q_2, q_3)^T \in \mathbb{R}^3$ and a scalar part $q_4 \in \mathbb{R}$, where the superscript T denotes the transpose of a vector:

$$\boldsymbol{q} = (\boldsymbol{e}^T, q_4)^T = \left(q_1, q_2, q_3, q_4\right)^T \tag{1}$$

By a unit quaternion $\boldsymbol{q}$, any given vector $\boldsymbol{r}\in\mathbb{R}^3$ in the reference frame can be rotated into the sensor frame:

$$\boldsymbol{b} = h(\boldsymbol{q}) = \boldsymbol{C}(\boldsymbol{q})\boldsymbol{r} \tag{2}$$

where $\boldsymbol{b}\in\mathbb{R}^3$ is the representation vector $\boldsymbol{r}$ in the sensor frame, and $\boldsymbol{C}(\boldsymbol{q})$ is the orientation matrix of the transformation from the reference frame to the sensor frame:

$$\boldsymbol{C}(\boldsymbol{q}) = (q_4^2 - \boldsymbol{e}^T\boldsymbol{e})\boldsymbol{I}_3 + 2\boldsymbol{e}\boldsymbol{e}^T - 2q_4[\boldsymbol{e}\times] \tag{3}$$

where $\boldsymbol{I}_3$ denotes 3×3 identity matrix, and the operator $[\boldsymbol{e}\times]$ represents the standard vector cross-product:

$$[\boldsymbol{e}\times] = \begin{pmatrix} 0 & -q_3 & q_2 \\ q_3 & 0 & -q_1 \\ -q_2 & q_1 & 0 \end{pmatrix} \tag{4}$$

Before the analysis it is necessary to define the coordinate systems. First, there exists a Global Coordinate System (GCS) which is earth related and time invariant. GCS is taken as the reference frame. Second, a Body Coordinate System (BCS) is attached to each body segment which is time variant coinciding with segment motion. The origin of each BCS is determined by the anatomical frame and is defined in the center of the functional axes as shown in Figure 3. Third, a Sensor Coordinate System (SCS) is defined by each sensor node itself and also coincides with segment motion. For the convenience of analysis, GCS, BCS, and SCS are also denoted as the reference frame, the body frame and the sensor frame, respectively. The estimated orientation quaternions are between GCS and SCS, denoted as $\boldsymbol{q}_t^{GS}$. The orientation quaternions employed by the displacement estimation are between GCS and BCS, denoted as $\boldsymbol{q}_t^{GB}$. The transformation from $\boldsymbol{q}_t^{GS}$ and $\boldsymbol{q}_t^{GB}$ can be performed by the initialization process.

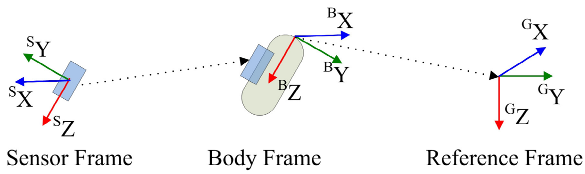

Fig. 3. The relationship between the sensor frame, the body frame and the reference frame

Orientation estimation is a difficult work in micro-sensor based motion capture systems. Li Gang (2009) presents an estimation method[8] using UKF algorithm, but he did not take characteristics of different signal sources into consideration. As a result disturbance from single source may bring huge error for the entire system. In consideration of different characteristics of the three signal source, namely acceleration, angular rate, earth magnetic field, our system use a multi-model orientation estimation method for data fusion[9]. The randomness of human motion brings random motions of sensor nodes, as a result of which could bring different disturbances for different types of sensor node: drift errors for gyroscope; human motion acceleration for accelerometer and iron disturbance for magnetometer. Such errors make degrees of confidence distinct between sensor types. Thus multi-models for orientation estimation should be considered.

Assuming that there are N_d models sharing the same dynamic model, namely $\{M_i\}_{i=1}^{N_d}$, the model probability $P\{M_i\}$ of the N_d models should satisfy: $P\{M_i\} \geq 0$ and $\sum_{i=1}^{N_d} P\{M_i\} = 1$.

In real-time orientation estimation, posterior probability of model M_i in node $j \in \{1, ..., N_s\}$ should be calculated, where N_s is the number of nodes and $i \in \{1, ..., N_d\}$. In our system $N_s = 16$ and $N_d = 4$. Thus the posterior probability of model M_i in node j can be evaluated by equation:

$$\mu_{i,t}^{(j)} = P\left\{M_{i,t}^{(j)} | \mathbf{Y}_t\right\} = \frac{1}{c^{(j)}} \Lambda_{i,t}^{(j)} \sum_{l=1}^{N_d} p_{li}^{(j)} \mu_{l,t-1}^{(j)} \tag{5}$$

$$c^{(j)} = \sum_{i=1}^{N_d} \Lambda_{i,t}^{(j)} \sum_{l=1}^{N_d} p_{li}^{(j)} \mu_{l,t-1}^{(j)} \tag{6}$$

where $i \in \{1, ..., N_d\}$ is index of different models;$j \in \{1, ..., N_s\}$ is node index; $\mathbf{Y}_t = \{\boldsymbol{y}_1, ..., \boldsymbol{y}_t\}$, $\boldsymbol{y}_t$ is the sensor observation in time t ; $M_{i,t}^j$ denotes that node j uses model i at time t . $\mu_{i,t}^{(j)}$ is posterior probability of model M_i in node j ; $p_{li}^{(j)}$ is the transforming probability form model l to model i :

$$p_{li}^{(j)} = P\left\{M_{i,t}^{(j)} | M_{l,t-1}^{(j)}, \mathbf{Y}_{t-1}\right\} \tag{7}$$

$\Lambda_{i,t}^{(j)}$ is the likelihood of model i in node j at time t:

$$\Lambda_{i,t}^{(j)} = P\left\{\boldsymbol{y}_t^{(j)} | M_{i,t}^{(j)}, \mathbf{Y}_{t-1}\right\} \tag{8}$$

To estimate accurate orientation, the likelihood and posterior probability mentioned above must be obtained. Assuming that orientation of model i in node j at time t is ${}^{GS}q_{i,t}^{(j)}$ and $i \in \{1, ..., N_d\}$, $j \in \{1, ..., N_s\}$, superscript GS denotes frame transformation from global frame to sensor frame. Quaternion q should satisfy:

$$\frac{d}{dt}\boldsymbol{q} = \frac{1}{2}\boldsymbol{\Omega}[\boldsymbol{\omega}]\boldsymbol{q} \tag{9}$$

where $\boldsymbol{\Omega}[\boldsymbol{\omega}]$ is a 4×4 skew matrix:

$$\boldsymbol{\Omega}[\boldsymbol{\omega}] = \begin{pmatrix} -[\boldsymbol{\omega}\times] & \boldsymbol{\omega} \\ -\boldsymbol{\omega}^T & 0 \end{pmatrix} \tag{10}$$

$\boldsymbol{\omega}$ is the angular velocity:

$$\boldsymbol{\omega} = \left(\omega_x, \omega_y, \omega_z\right)^T \tag{11}$$

operator $[\boldsymbol{\omega}\times]$ represents the standard vector cross-product in equation (4).

Among three type of measurement units, gyroscope measures angular rate mixed with bias and noise, the observation of node $j \in \{1, ..., N_s\}$ is:

$$\boldsymbol{y}_{G,t}^{(j)} = \boldsymbol{\omega}_t^{(j)} + \boldsymbol{h}_{G,t}^{(j)} + \boldsymbol{v}_{G,t}^{(j)} \tag{12}$$

where G, t means gyroscope observation at time t ; $\boldsymbol{v}_{G,t}^{(j)}$ is gyroscope noise, assuming zero-mean Gaussian noise following distribution $N(\mathbf{0}, \boldsymbol{\Sigma}_G^{(j)})$ here; $\boldsymbol{h}_{G,t}^{(j)}$ is bias vector. As bias of gyroscope varies slowly with respect to its observation, we model $\boldsymbol{h}_{G,t}^{(j)}$ as a random walk model:

$$\boldsymbol{h}_{G,t}^{(j)} = \boldsymbol{h}_{G,t-1}^{(j)} + \boldsymbol{w}_{h,t}^{(j)} \tag{13}$$

where $\boldsymbol{w}_{h,t}^{(j)}$ is zero-mean Gaussian white noise.

Then we can get dynamic system equation: system state vector $\boldsymbol{x}_{i,t}^{(j)}$ of model i in node j at time t consists of quaternion ${}^{GS}\boldsymbol{q}_{i,t}^{(j)}$ and bias $\boldsymbol{h}_{G,t}^{(j)}$:

$$\boldsymbol{x}_{i,t}^{(j)} = \begin{pmatrix} {}^{GS}\boldsymbol{q}_{i,t}^{(j)} \\ \boldsymbol{h}_{G,t}^{(j)} \end{pmatrix} \tag{14}$$

the state equation is:

$$\begin{aligned} \boldsymbol{x}_{i,t}^{(j)} &= f_{i,t}^{(j)}\left(\boldsymbol{x}_{i,t}^{(j)}\right) + \boldsymbol{w}_{i,t}^{(j)} \\ &= \begin{pmatrix} \exp\left(\frac{1}{2}\boldsymbol{\Omega}[\boldsymbol{y}_{G,t}^{(j)} - \boldsymbol{h}_{G,t}^{(j)}]\Delta\right) & \boldsymbol{O}_{4\times 3} \\ \boldsymbol{O}_{3\times 4} & \boldsymbol{I}_3 \end{pmatrix} \cdot \boldsymbol{x}_{i,t}^{(j)} + \begin{pmatrix} \boldsymbol{w}_{q,i,t}^{(j)} \\ \boldsymbol{w}_{h,t}^{(j)} \end{pmatrix} \end{aligned} \tag{15}$$

The observation of gyroscope is the input of system dynamic model, as a result of which quaternion orientation estimation is updated using real-time observation without any lag.

Among three types of measurement units, magnetometers measure earth magnetic field mixed with noise and magnetic distortion:

$$\boldsymbol{y}_{M,t}^{(j)} = \boldsymbol{B}_{M,t}^{(j)} + \boldsymbol{H}_{M,t}^{(j)} + \boldsymbol{V}_{M,t}^{(j)} \tag{16}$$

where M, t denotes magnetometer observation at time t ; $\boldsymbol{V}_{M,t}^{(j)}$ is observation noise of magnetometers; $\boldsymbol{H}_{M,t}^{(j)}$ is magnetic distortion caused by soft or hard iron disturbances; $\boldsymbol{B}_{M,t}^{(j)}$ is earth magnetic field vector on sensor frame.

Noticed that $\boldsymbol{y}_{M,t}^{(j)}$ consists of magnitude as well as direction information, and only direction useful for orientation estimation. Furthermore, its magnitude information may lead error in orientation estimation. Thus normalization of equation (16) should be performed. Moreover, for the sake of multi-model estimation, bias $\boldsymbol{H}_{M,t}^{(j)}$ should be put into noise:

$$\boldsymbol{z}_{M,i,t}^{(j)} = \boldsymbol{b}_{M,i,t}^{(j)} + \boldsymbol{v}_{M,i,t}^{(j)} \tag{17}$$

where $\boldsymbol{v}_{M,i,t}^{(j)}$ is normalized magnetometer observation noise of model i in node j at time t , which is modeled as Gaussian distribution $N(\mathbf{0}, \boldsymbol{\Sigma}_M^{(j)})$; $\boldsymbol{b}_{M,i,t}^{(j)}$ is earth magnetic field vector on sensor frame. Given a quaternion $\boldsymbol{q}_{i,t}^{(j)}$ and earth magnetic field vector on certain frame $\boldsymbol{r}_M$, magnetometer measurement $\boldsymbol{b}_{M,i,t}^{(j)}$ should be evaluated through:

$$\boldsymbol{b}_{M,i,t}^{(j)} = \boldsymbol{C}\left(\boldsymbol{q}_{i,t}^{(j)}\right) \cdot \boldsymbol{r}_M \tag{18}$$

Thus observation equation of magnetometer is:

$$\boldsymbol{z}_{M,i,t}^{(j)} = \boldsymbol{C}\left(\boldsymbol{q}_{i,t}^{(j)}\right) \cdot \boldsymbol{r}_M + \boldsymbol{v}_{M,i,t}^{(j)} \tag{19}$$

Similarly, for accelerometer we have:

$$\boldsymbol{y}_{A,t}^{(j)} = \boldsymbol{C}\left(\boldsymbol{q}_{i,t}^{(j)}\right) \cdot \boldsymbol{r}_A + \boldsymbol{H}_{A,t}^{(j)} + \boldsymbol{V}_{A,t}^{(j)} \tag{20}$$

where A,t denotes accelerometer observation at time t ; $\boldsymbol{V}_{A,t}^{(j)}$ is observation noise of accelerometer; $\boldsymbol{H}_{A,t}^{(j)}$ is human motion acceleration; $\boldsymbol{r}_A$ is earth gravity acceleration measurement on sensor frame.

Noticed that $\boldsymbol{y}_{A,t}^{(j)}$ consists of magnitude as well as direction information, and only direction useful for orientation estimation. Furthermore, its magnitude information may lead error in orientation estimation. Thus normalization of equation (20) should be performed. Moreover, for the sake of multi-model estimation, bias $\boldsymbol{H}_{A,t}^{(j)}$ should be put into noise:

$$\boldsymbol{z}_{A,i,t}^{(j)} = \frac{\boldsymbol{y}_{A,t}^{(j)}}{g} = \boldsymbol{C}\left(\boldsymbol{q}_{i,t}^{(j)}\right)\left(\frac{\boldsymbol{r}_A}{g}\right) + \boldsymbol{v}_{A,i,t}^{(j)} \tag{21}$$

where $\boldsymbol{v}_{A,i,t}^{(j)}$ is normalized accelerometer observation noise of model i in node j at time t , which is modeled as Gaussian distribution $N(\mathbf{0}, \boldsymbol{\Sigma}_A^{(j)})$; g is earth gravity acceleration vector on sensor frame.

Then, system observation equation could be conducted. Assume that system observation is $\boldsymbol{z}_{i,t}^{(j)}$:

$$\begin{aligned} \boldsymbol{z}_{i,t}^{(j)} &= \begin{pmatrix} \boldsymbol{z}_{M,i,t}^{(j)} \\ \boldsymbol{z}_{A,i,t}^{(j)} \end{pmatrix} = g_{i,t}^{(j)}\left(\boldsymbol{x}_{i,t}^{(j)}\right) + \boldsymbol{v}_{i,t}^{(j)} \\ &= \begin{pmatrix} \boldsymbol{C}(\boldsymbol{q}_{i,t}^{(j)}) & \boldsymbol{O}_{3\times 3} \\ \boldsymbol{O}_{3\times 3} & \boldsymbol{C}(\boldsymbol{q}_{i,t}^{(j)}) \end{pmatrix} \cdot \begin{pmatrix} \boldsymbol{r}_M \\ \frac{\boldsymbol{r}_A}{g} \end{pmatrix} + \begin{pmatrix} \boldsymbol{v}_{M,i,t}^{(j)} \\ \boldsymbol{v}_{A,i,t}^{(j)} \end{pmatrix} \end{aligned} \tag{22}$$

Assuming that $\boldsymbol{v}_{M,i,t}$ does not correlate with $\boldsymbol{v}_{A,i,t}$, system observation noise covariance matrix $\boldsymbol{R}_t = \begin{pmatrix} \boldsymbol{\Sigma}^{(j)}_{M,i,t} & \boldsymbol{O}_{3\times3} \\ \boldsymbol{O}_{3\times3} & \boldsymbol{\Sigma}^{(j)}_{A,i,t} \end{pmatrix}$

Using equation (22) and (15) $\mu^{(j)}_{i,t} = P\left\{M^{(j)}_{i,t}|\boldsymbol{Y}_t\right\}$ could be evaluated. The final orientation ${}^{GS}\boldsymbol{q}^{(j)}_t$ is estimated through:

$$ {}^{GS}\boldsymbol{q}^{(j)}_t = \sum_{i=1}^{N_d} {}^{GS}\boldsymbol{q}^{(j)}_{i,t} \cdot \mu^{(j)}_{i,t} \tag{23} $$

5 Experimental Results

Experiment investigates the accuracy of our orientation system in contrast with optical motion capture system. As is shown in Fig 4, human lower limbs movements are captured by our MMocap system and Osprey optical system[10]. Osprey optical system captures human motion using six cameras in 2m × 3m space. In our contrast experiment, optical markers and micro-sensors are fixed on human waist, thigh and calf, and both systems capture human motion with 100Hz sample rate. There are three scenes in our experiments:

1. *Scene I:* running forward, backward and jump aside repeatedly with left, right and back turning.
2. *Scene II:* jumping forward repeatedly with back turning.
3. *Scene III:* walking forward, backward and step aside repeatedly with left, right and back turning.

Each scene are sample over 30s for over 5 times. For the convenience of evaluation, quaternions from fusion methods are transformed into degrees. The estimation

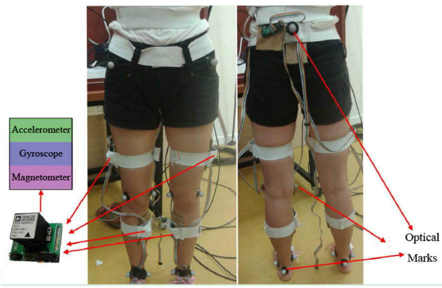

Fig. 4. Contrast experiment between our system and optical system

Table 1. RMSE of MMocap System: mean *pm* standard deviation

Scene	Scene I	Scene II	Scene III
Angle (deg)	2.66 ± 2.56	2.42 ± 1.84	2.44 ± 2.34
Displacement (m)	0.0707 ± 0.0469	0.1673 ± 0.0656	0.0990 ± 0.0374

RMSE of MMocap system to optical system is summarized in Table 1. It can be seen that, unlike other methods, the orientation error of our method does not increase much when the motion acceleration grows. From the comparison of these results, our algorithm has shown its accuracy, stability and efficiency.

Acknowledgement. This paper is supported by the National Natural Science Foundation of China (Grant No. 60932001), and partially supported by CSIDM project 200802.

References

1. Vicon, `http://www.vicon.com`
2. Gypsy Motion Capture System, `http://www.metamotion.com`
3. Vlasic, D., Adelsberger, R., Vannucci, G., Barnwell, J., Gross, M., Matusik, W., Popovic, J.: Practical motion capture in everyday surroundings. ACM Transactions on Graphics (TOG) 26(3) (July 2007)
4. Verhaert's ALERT system, `http://www.verhaert.com/`
5. MotionStar Motion Capture System, `http://www.vrealities.com/motionstar.html`
6. Priyantha, N., Chakraborty, A., Balakrishnan, H.: The cricket location-support system. In: International Conference on Mobile Computing and Networking, pp. 32–43 (2000)
7. Randell, C., Muller, H.: Low Cost Indoor Positioning System. In: Abowd, G.D., Brumitt, B., Shafer, S.A.N. (eds.) UbiComp 2001. LNCS, vol. 2201, pp. 42–48. Springer, Heidelberg (2001)
8. Li, G., Wu, Z., Wu, J.-K.(n.d.): Micro-sensor driven human model for 3D real-time movement. Journal of Computer Applications 12 (2009)
9. Chen, J., Sun, S., Tao, G., Wu, J. (n.d.): Multi-model Orientation Estimation by Fusion of Micro Sensory Data. Measurement, 4–7
10. Osprey System, `http://www.motionanalysis.com/html/movement/osprey.html`